JOC The Journal of Organic Chemistry

pubs.acs.org/joc Article

Photovermellogens: Minimalistic Pyridinium-Based Acylhydrazones with Photoswitchable Basicity for Operation in Aqueous Media

Alejandro Vila, Francisco G. Blandón-Cumbreras, Mike Pauls, Mauro Díaz-Abellás, Arturo Blanco-Gómez, Carlos Peinador, Patricia Remón, Christoph Bannwarth,* Uwe Pischel,* and Marcos D. García*

Cite This: J. Org. Chem. 2026, 91, 6559−6565

ABSTRACT: Examples of a new class of synthetically straightforward and hydrolytically inert photoswitchable acylhydrazones, named photovermellogens, have been successfully developed and comprehensively studied using state-of-the-art spectroscopic and computational techniques. These compounds present photoswitchable basicity, with irradiation promoting $E \rightarrow Z$ photoisomerizations, which result in the generation of a less acidic species. The observed ΔpK_a values > 1.5 within the biologically relevant window underscore the potential of photovermellogens as versatile platforms for light-triggered pH control.

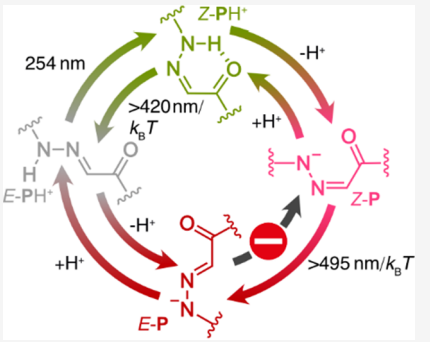

1. INTRODUCTION

Molecular photoswitches (MPs)[1] are key tools in modern chemistry,[2] with light stimulation enabling the precise spatiotemporal and remote noninvasive manipulation of matter.[3] However, analogues capable of efficiently operating in biological milieus remain underdeveloped.[4] Considering the different strategies for enhancing aqueous solubility, the introduction of ionizable groups is of particular interest, as such systems can also undergo a pK_a shift upon photoisomerization, showing photoswitchable acidity/basicity,[5] opening the door for applications that rely on light-induced pH modulations.[6]

Among the popular families of MPs,[1−6] (acyl)hydrazones hold particular promise as extensively proven by Aprahamian et al.[7] First, their appropriate functionalization leads to controlled photoisomerization of the C═N bond, and/or fine-tuning of the E/Z populations. Furthermore, the ability of these species to establish multifaceted noncovalent interactions, allows for further adjustment of the responsiveness by hydrogen bonding (HB) or anion/cation coordination.[8] Finally, the photochemical properties have been thoroughly investigated, demonstrating favorable photostationary distributions (PSDs), high fatigue resistance, significant quantum yields and modular thermal half-lives. Despite these desirable features, the often limited and pH-dependent hydrolytic stability of imine derivatives[9] poses a significant drawback and thus, only a few examples of (acyl)hydrazone photoswitching in aqueous environments have been reported.[10]

In this context, some of us have reported the development of vermellogens (Scheme 1),[11] pH-responsive analogues of the well-known viologens,[12] that feature the insertion of a hydrazone function between two pyridinium rings. Previously, we found that the positively charged heterocycles not only enable water solubility, but also act as electron density sinks for the hydrazone group, increasing the hydrolytic stability of the C═N bond,[9] and producing unusually low pK_a values for the NH motif in the range of 6−12.[11,13,14] Herein we present the evolution of the functionality of vermellogens into the proposed dual pH-/light-responsiveness of photovermellogens $\mathbf{P}_{a-d}H^+$.[15] As shown in Scheme 1, the high acidity of the hydrazone in vermellogens is proposed to be potentially preserved by using a 4-hydrazinylpyridinium-like scaffold in the readily accessible analogues $\mathbf{H}_{a-d}^+$ that were used as synthetic precursors.[16] In turn, condensation of these intermediates with phenyl glyoxal in acidic aqueous medium introduces a carbonyl group in α-position to the C═N bond, aimed to stabilize the otherwise minor Z isomers by HB and thereby promote E to Z photoswitching.[7] Hence, our designed compounds can potentially exist in four different states E/Z-[$\mathbf{P}_{a-d}/\mathbf{P}_{a-d}H^+$], depending on the degree of protonation of the NH group and the E/Z isomerization of the C═N bond.

Received: November 24, 2025
Revised: April 7, 2026
Accepted: April 17, 2026
Published: May 4, 2026

https://doi.org/10.1021/acs.joc.5c02962
J. Org. Chem. 2026, 91, 6559−6565

Scheme 1. From Viologens to Photovermellogens[a]

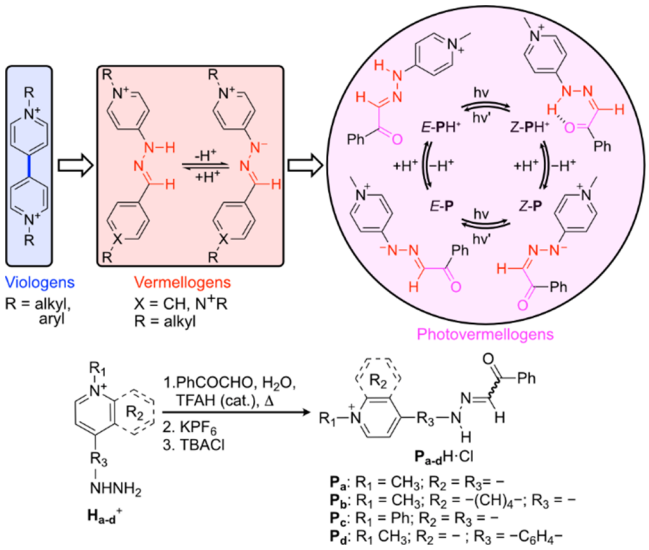

[a]Top: Structural evolution into photovermellogens. Bottom: Synthesis of photovermellogens.

2. RESULTS AND DISCUSSION

2.1. Synthesis and Structural Characterization

Regarding the synthesis of the intended compounds, the employed reaction conditions induced in all cases the quantitative self-assembly of the reactants into single products. This end was corroborated by ^{1}H NMR monitoring, which conveniently showed the disappearance of the reactants, and the advent of the diagnostic HC═N resonances for the acylhydrazone moiety at δ = 7.0–8.5 ppm (Figure S1, S1). The targeted water-soluble salts $\mathbf{P}_{a-d}$H·Cl were obtained in good yields, by precipitating the cations from the reaction mixture with KPF_6, and subsequent ion metathesis with Bu_4NCl. All compounds "as-synthesized" were extensively characterized by 1D/2D NMR (Figure 1a) and HR-ESI MS.[16] Except for $\mathbf{P}_d$H·PF_6/Cl (isolated as an 89/11 mixture of *E*/*Z* isomers), the other salts were obtained solely as the corresponding *E* forms, with NOESY NMR experiments in organic media showing defined NOE peaks between the *syn*-periplanar protons on the HC═N–NH moieties (Figure 1b). Further structural evidence for the identity of all compounds but $\mathbf{P}_d$H·PF_6/Cl, was obtained by SC-XRD, with the cations in the solid state showing both the *E* configuration of the C═N bond, and a preferred *syn* disposition of the carbonyl group regarding the HC═N proton (Figure 1a). All obtained compounds were stored as solids in the refrigerator, protected from light. No signs of degradation were observed after long time storage (1 year). In solution, the compounds remained stable in the dark with no significant changes of the spectroscopic features being observed after 1 week at pD 5.5 (Figures S126–S129, SI1). This implies high hydrolytic stability, as inferred from our design rationale.

2.2. Stimuli-Responsiveness

With the photovermellogens synthesized and fully characterized, their acid–base properties were next investigated by UV–vis spectroscopy to determine whether the pH-responsiveness characteristic of parent vermellogens was retained. Indeed, $\mathbf{P}_{a-d}$H·Cl reproduced the archetypical absorption changes of

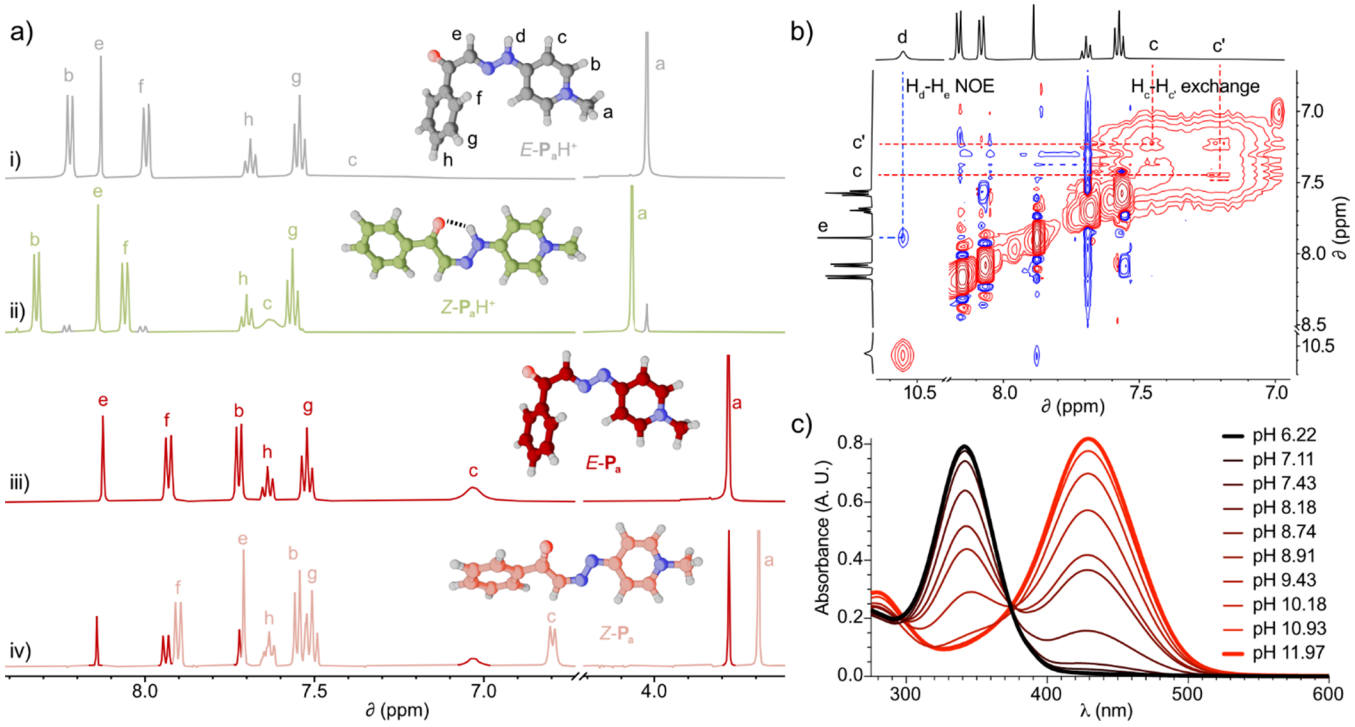

Figure 1. Spectroscopic features of photovermellogens, exemplified for $\mathbf{P}_a$H·Cl: (a) ^{1}H NMR spectra (500 MHz, D_2O) for 5 mM *E*-$\mathbf{P}_a$H·Cl: (i) pD = 6; (ii) irradiation at 254 nm, pD 6; (iii) pD 12; and (iv) irradiation at 254 nm, followed by adjustment of pD to 13.[17] The main species in each spectrum are represented by representative geometries obtained from (i): SC-XRD data and (ii–iv): optimization at the density functional theory level (PBEh-3c+CPCM).[18,19] Color code: H (light gray), N (blue), and O (red). Carbon atoms are color-coded according to isomer and protonation state as gray [*E*-$\mathbf{P}_a$H$^+$], green [*Z*-$\mathbf{P}_a$H$^+$], dark red [*E*-$\mathbf{P}_a$], and salmon [*Z*-$\mathbf{P}_a$]. (b) Partial EXSY/NOESY NMR spectra (CD_3CN, 500 MHz) for *E*-$\mathbf{P}_a$H·PF_6. (c) UV–vis spectra of 20 μM *E*-$\mathbf{P}_a$H·Cl in buffered solutions of varying pH.

https://doi.org/10.1021/acs.joc.5c02962
J. Org. Chem. 2026, 91, 6559–6565

Table 1. Relevant Physicochemical Data for $P_{a-d}H$·Cl in water

	pK_a (*E*-PH$^+$)[a]	pK_a (PSD)[b]	λ_{max}/ nm[c] (*E*-PH$^+$) [ε/ M^{-1}·cm^{-1}][d]	λ_{max}/nm[c] (*Z*-PH$^+$) [ε/ M^{-1}·cm^{-1}][d]	λ_{max}/ nm[c] (*E*-P) [ε/ M^{-1}·cm^{-1}][d]	λ_{max}/ nm[c] (*Z*-P) [ε/ M^{-1}·cm^{-1}][d]	$\Phi_{E\to Z}$[e]	PSD[f] *E*→*Z*	$\Phi_{Z\to E}$[e]	PSD[f] *Z*→*E*	$k_{Z\to E}$[g] (10^{-4} s^{-1})
P_aH^+	8.8 ± 0.2	10.4 ± 0.2	342 [41,000]	352 [43,000]	429 [39,000]	420 [18,000]	0.20	93% *Z*	0.001	67% *E*	4.1
P_bH^+	7.2 ± 0.1	8.8 ± 0.2	378 [42,000]	384, [36000]	456 [42,000]	445 [13,000]	0.38	93% *Z*	0.002	57% *E*	9.8
P_cH^+	7.8 ± 0.1	9.9 ± 0.1	349 [49,000]	359 [43,000]	432 [46,000]	420 [15,000]	0.34	98% *Z*	0.008	55% *E*	2.4
P_dH^+	11.2 ± 0.1	–[h]	411 [66,000]	–[h]	500 [69,000]	–[h]	–[h]	–[h]	–[h]	–[h]	–[h]

[a]Acidity constant of the cationic *E* form. [b]Apparent acidity constant of the cationic *Z* form, as present in the photostationary state (88–97% *Z*). [c]Maximum of the longest-wavelength absorption band. [d]Molar absorption coefficient; error ± 5%. [e]Photoisomerization quantum yield for irradiation at 254 nm (*E*→*Z*) or 440 nm (*Z*→*E*) at pH 6; error ± 20%. The quantum yields for *E*→*Z* isomerization upon irradiation at 365 nm are very similar: P_aH^+ – 0.22, P_bH^+ – 0.35, P_cH^+ – 0.34. [f]Photostationary state distribution (PSD) upon irradiation at 254 nm (*E*→*Z*) or >420 nm (*Z*→*E*) at pD 6. The PSD for upon irradiation at 365 nm (*E*→*Z*) are marginally smaller: P_aH^+ – 87% *Z*, P_bH^+ – 92% *Z*, P_cH^+ – 93% *Z*. [g]Unimolecular rate constant for the thermal back-isomerization upon heating to 60 °C (P_aH^+ at pD 6) or 70 °C (P_bH^+ at pD 5; P_cH^+ at pD 6). [h]No data obtained due to the lack of photoisomerization.

vermellogens (Figures 1c and S130–S137, SI1).[11,13,14] In essence, the characteristic intense π–π^* absorption bands of the cations undergo a considerable bathochromic shift upon deprotonation (Table 1), as also confirmed by our quantum chemical calculations (Figure S2, S2),[16] causing a notable color change from yellow to red. This pronounced shift allowed the estimation of pK_a values for *E*-$P_{a-d}H^+$ *via* UV–vis absorption titrations, which, as for other vermellogens, fall within the biologically relevant pH range (Figure 1c, Table 1 and Figures S130–S137, SI1). Changes in the protonation state were also easily monitored by ^{1}H NMR spectroscopy, with the gain in electronic density translating in a substantial shielding of resonances of the corresponding conjugate bases *E*/*Z*-P_{a-d} (Figure 1a).[17] As already observed for *E*-$P_{a-d}H^+$, the deprotonated species were also thermally stable in the absence of light.

The knowledge of the pK_a values enabled the decoupling of acid–base effects from the investigation of the light-responsiveness of photovermellogens. These effects were separately examined for $P_{a-d}H^+$ and their conjugate bases, each appropriately prepared by dissolving the "as-synthesized" salts in buffered solutions at pH = pK_a ± 2.

Photoisomerization studies were subsequently carried out in acidic medium (pH = pK_a – 2) in order to assess the photoresponse of the protonated species. Under these conditions, the anticipated photoisomerization of the thermally stable *E*-$P_{a-d}H^+$ species was investigated by UV–vis absorption spectroscopy under irradiation at 254 nm. Except for *E*-P_dH^+, which showed no detectable changes, irradiation promoted the formation of *Z*-$P_{a-c}H^+$ isomers, evidenced by a gradual red shift of the π–π^* absorption band and the expected first-order kinetic behavior of the processes (Figures 2a and S138–S143, SI1).[16] Consistent with related (acyl)hydrazone-based switches,[7−10] the photoreactions displayed quantum yield of 0.2–0.4 and reached excellent photostationary-state distributions (≈95%), as verified by relative integration of diagnostic ^{1}H NMR signals (Figure 1a and S149–S154, SI1). It is noteworthy that the irradiation wavelength can be extended to 365 nm, yielding virtually the same observations as for 254 nm irradiation (see footnotes of Table 1).[16] Irradiation also produced clear NMR spectral changes that support the occurrence of the *E*→*Z* isomerization. In essence, the signals H_{f-h} of the phenyl moiety were only slightly affected, whereas those of the pyridinium and acylhydrazone fragments shifted markedly, consistent with the formation of an intramolecular hydrogen bond in the *Z*-$P_{a-c}H^+$ species. The reverse *Z*→*E* transformation of the protonated forms $P_{a-c}H^+$ was also achieved upon irradiation at λ > 420 nm,

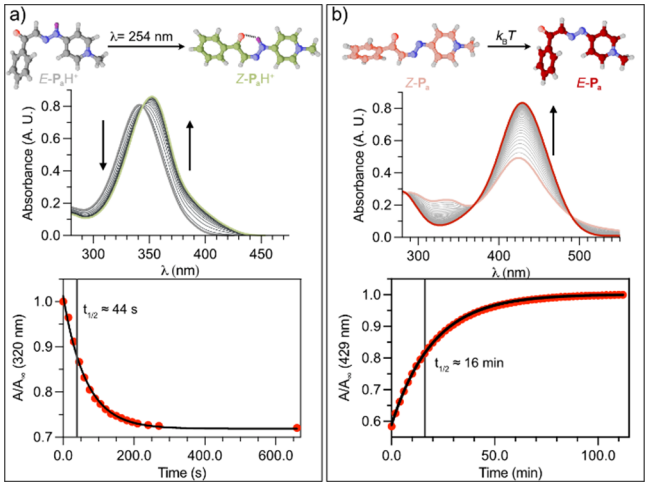

Figure 2. (a) Variation over time of the absorption spectrum of *E*-P_aH·Cl (21 μM, pH = 6) upon irradiation at 254 nm, and fitting of the absorbance ratio at 320 nm vs time to first-order kinetics. (b) Variation over time of the absorption spectrum at r.t. of a *Z*-P_a-enriched solution at pH 13 (prepared as described in the main text), and fitting of the absorbance ratio at 429 nm vs time to a first-order kinetics.

giving lower quantum yields and less favorable PSDs (Figures S145–S147, S149–154, S1). Thermal reversion can occur as well, however, in a significantly slower time scale as indicated by the measured rate constants (Table 1 and Figures S155–S159, SI1). For the example of *Z*-P_aH^+ the activation energy was determined as E_A = 17.4 kcal·mol^{-1} and a half-life of the *Z* form of ca. 9 h at room temperature (298 K) was extrapolated (Figures S156–S157, SI1).

Having confirmed the photochemical behavior of the protonated forms, we next explored their light-responsiveness in the deprotonated state. Following the same procedure used for their cationic counterparts, the neutral *E*-P_{a-d} species were investigated in basic media (pH = pK_a + 2), where photoisomerization studies showed a markedly different behavior. While *E*-$P_{a-c}H^+$ exhibited the dual photochemical features of P-/T-type switches (see above),[1] the corresponding conjugate base *E*-P_{a-c} showed no detectable *E*→*Z* conversion upon irradiation (Figures S160–S162, SI1).[20] To probe whether *Z*-P_{a-c} could nonetheless be generated indirectly, we explored a consecutive photoisomerization–deprotonation sequence. Thus, *E*-$P_{a-c}H^+$ was first irradiated at 254 nm and pH 6 to enrich the *Z* population, followed by immediate adjustment of the solution to pH 13. Under these conditions, transient

https://doi.org/10.1021/acs.joc.5c02962
J. Org. Chem. 2026, 91, 6559–6565

spectroscopic features were observed, consistent with the kinetic trapping of the metastable *Z*-$\mathbf{P}_{a-c}$ species. UV−vis spectra displayed similar maxima and bathochromic shifts to those of the deprotonated *E*-isomers (Table 1 and Figures S163−S168, SI1).[20] More revealingly, the ^{1}H NMR spectra exhibited two distinct sets of signals in slow exchange on the NMR time scale, consistent with *E*/*Z* mixtures of the corresponding conjugate bases (Figure 1a). The signals attributable to the new species were assigned by COSY experiments, which confirmed both the expected multiplicity and relative integration for *Z*-$\mathbf{P}_{a-c}$ (Figures S41, S75 and S105 SI1) and revealed a clear deprotonation-induced shielding compared to *Z*-$\mathbf{P}_{a-c}H^+$. These spectroscopic observations enabled the estimation of virtual pK_a values for the *Z*-enriched solutions (Table 1 and Figures S163−168, SI1), which confirmed the reduced acidity of the NH group in the *Z*-isomers, presumably arising from intramolecular hydrogen-bond formation.

To gain further insight into the behavior of the metastable *Z*-bases, absorbance changes of the kinetically trapped state were monitored over time in the dark for the whole $\mathbf{P}_{a-c}$ series. In all cases, the data fitted well to the expected unimolecular kinetics for thermally induced *Z*→*E* processes (Figures 2b, S169, S171−S172, SI1). Notably the thermal half-life increased dramatically upon substitution, from ca. 16 min for $\mathbf{P}_a$ to several hours for $\mathbf{P}_b$ and $\mathbf{P}_c$. Using $\mathbf{P}_a$H·Cl as a representative model, the photochemically induced back-isomerization was additionally investigated under irradiation at λ > 495 nm (Figure S170, SI1), revealing that the photo- and thermally induced *Z*→*E* processes operate on comparable time scales, with the thermal pathway being slightly slower.

Overall, the experimental results for the $\mathbf{P}_{a-c}$H·Cl series reveal a behavior characteristic of photoswitches with light-responsive basicity, where *E*→*Z* photoisomerization drives a reversible shift in pK_a between two ground-state forms.[5,6] In acidic medium, the protonated species $\mathbf{P}_{a-c}H^+$ display the typical features of acylhydrazone-type photoswitches, combining both P-/T-type responses.[1] Upon deprotonation, however, the conjugate bases $\mathbf{P}_{a-c}$ lose their ability to undergo the forward *E*→*Z* photoisomerization. This contrasting photoresponse is assigned to the intramolecular C═O···H−N HB motif, which is essential for an efficient *E*→*Z* conversion.

2.3. Computational Study

To further rationalize the photochemical properties of photovermellogens at the molecular level we performed quantum-mechanical calculations on $\mathbf{P}_aH^+$ as a representative model (see SI2 for details and expanded discussion). We first investigated the photoisomerization mechanism of the acidic form of the species (Figure 3). As shown, at the experimental irradiation conditions (λ = 254 nm), the bright S_2 state (π→π*) of *E*-$\mathbf{P}_aH^+$ becomes populated. From there, an S_1/S_2 minimum energy conical intersection (MECI) that involves a barrier of about 5.0 kcal·mol^{-1} with respect to a local S_2 minimum, enables progression to the n→π* S_1 excited state ($\theta \sim 133°$). The *E*-isomer can either relax to the n→π* S_1, which eventually relaxes back to the ground state, or convert to the *Z*- form passing a S_0/S_1 MECI ($\theta \sim 90°$, schematic red path in Figure 3). This step involves a negligible barrier of just 0.3 kcal·mol^{-1} relative to the S_1 minimum, and poses one path for *E*→*Z* photoisomerization. Since the n→π* state is essentially dark, with a computed oscillator strength of f_{01} = 0.00, it is unlikely to be efficiently populated by irradiation, and the excited-state trajectory is expected to start from S_2. One should note that the relative

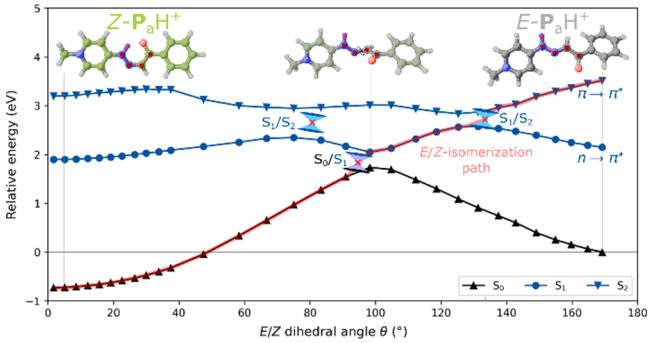

Figure 3. Potential energy curve (hh-TDA[21,22]-PBEh-3c[18,23]//GFN2-xTB[24]+ALPB[25]) along the *E*/*Z*-isomerization coordinate θ of $\mathbf{P}_aH^+$ for the ground state S_0 (black upper triangles) and the singlet excited states S_1 (blue circles) and S_2 (blue lower triangles). Relevant minimum energy conical intersections (see SI2 for details) and a possible photoisomerization pathway (red, dashed line) are displayed.

ground-state stability of the *Z*/*E*-isomers in Figure 3 is inverted when a variational, solvation-inclusive theory level is used (Table 1, SI2). In that case, the *E*-form is more stable by about 2 kcal·mol^{-1}. Nevertheless, the inverted ground-state energetics from the hh-TDA[21,22] calculations (Figure 3), is not expected to affect the interpretation of the photoisomerization mechanism based on the S_1 and S_2 state surfaces.

We performed an analogous set of calculations to characterize the deprotonated form $\mathbf{P}_a$.[16] Associated with the observed red shift is the fact that now the visible π→π* becomes lowest in energy. This state is mostly comprised of contributions from the highest occupied molecular orbital (HOMO) and lowest unoccupied molecular orbital (LUMO). Given that the HOMO−LUMO energy gap is notably smaller for the deprotonated form $\mathbf{P}_a$, this rationalizes its pronounced red-shifted absorption as compared to the protonated form. These changes in the π→π* states are also recognizable looking at the natural transition orbitals (NTOs)[26] given in Figures S2−S3 in SI2. We identified MECIs comparable to those of $\mathbf{P}_aH^+$, which suggest photoisomerization to be feasible. However, there exists no structural motif which would prevent back isomerization to *E*-$\mathbf{P}_a$. While the calculated barrier for thermal *E*/*Z*-isomerization $\Delta G^{\ddagger}$ are clearly very high in free energy, we still find a notable decrease for $\mathbf{P}_a$ (33.0 kcal·mol^{-1}) over $\mathbf{P}_aH^+$ (43.6 kcal·mol^{-1}). $\Delta G^{\ddagger}$ of $\mathbf{P}_a$ is similar in size to results known for other hydrazone photoswitches in literature,[27,28] and resembles an inversion-type double bond rotation. On the other hand, thermal isomerization in the protonated form $\mathbf{P}_aH^+$ is associated with an adiabatic rotation-type transition state. While this is more similar to azobenzene, the possibility of a nonadiabatic rotation-type isomerization as found for azobenzene,[28] was not explored in the present work, but certainly deserves more attention in the future.

3. CONCLUSIONS

The experimental and computational results converge into a coherent picture, in which protonation controls the efficiency and metastability of photovermellogens. Protonated species $\mathbf{P}_{a-c}H^+$ behave as P/T-type acylhydrazone switches, while deprotonation disrupts the hydrogen-bond motif that enables *E*→*Z* photoisomerization, allowing only *Z*→*E* relaxation. Calculations support this mechanism, showing low-barrier excited-state crossings for $\mathbf{P}_aH^+$ and destabilization of the *Z*-form upon deprotonation. Overall, photovermellogens constitute a new class of synthetically straightforward accessible and

https://doi.org/10.1021/acs.joc.5c02962
J. Org. Chem. 2026, 91, 6559−6565

modular acylhydrazone-based photoswitches, which uniquely combine hydrolytic stability with tunable photochemical and acid–base properties. Their high resistance to hydrolysis, conferred by the electron-withdrawing pyridinium framework, ensures reliable operation in aqueous environments—a feature that remains challenging for many (acyl)hydrazone systems.[9] Displaying photoswitchable basicity, they provide a distinct platform for light-induced pH modulation in water through $E \rightarrow Z$ photoisomerization, extending aqueous photobase chemistry beyond spiropyrans[29] and related families.[4] Owing to their favorable properties, photovermellogens emerge as promising, water-compatible scaffolds for next-generation molecular photoswitches.

4. SAFETY STATEMENT

No unexpected or significant hazards beyond those commonly encountered in routine synthetic chemistry were identified during this work. The compounds described herein should be handled with care, avoiding inhalation and skin or eye contact. All procedures were conducted in a well-ventilated fume hood. No unexpected or significant hazards beyond those commonly encountered in routine synthetic chemistry were identified.

■ ASSOCIATED CONTENT

Data Availability Statement

The data underlying this study are available in the published article and its Supporting Information.

Supporting Information

The Supporting Information is available free of charge at https://pubs.acs.org/doi/10.1021/acs.joc.5c02962.

SI1: Experimental details, synthetic procedures and characterization data for new compounds, hydrolytic stabilities, titration data for the determination of pK_a values, isomerization photochemical data, crystallographic data for *E*-$\mathbf{P_a}$H·PF_6, *E*-$\mathbf{P_b}$H·I and *E*-$\mathbf{P_c}$H·PF_6 (CCDC: 2486929, 2487028 and 2486961, respectively), and additional figures (PDF)

SI2: Computation of free energies, absorption spectra, and thermal and complementary data for thermal isomerization and photoisomerization (PDF)

SI3: Coordinates for all computed structures and outputs of quantum chemical calculations (ZIP)

Accession Codes

Deposition Numbers 2486929, 2486961, and 2487028 contain the supplementary crystallographic data for this paper. These data can be obtained free of charge via the joint Cambridge Crystallographic Data Centre (CCDC) and Fachinformationszentrum Karlsruhe Access Structures service.

■ AUTHOR INFORMATION

Corresponding Authors

Christoph Bannwarth − *Institute of Physical Chemistry, RWTH Aachen University, Aachen 52074, Germany;* orcid.org/0000-0003-3242-496X; Email: bannwarth@pc.rwth-aachen.de

Uwe Pischel − *CIQSO − Center for Research in Sustainable Chemistry and Department of Chemistry, University of Huelva, Huelva 21071, Spain;* orcid.org/0000-0001-8893-9829; Email: uwe.pischel@diq.uhu.es

Marcos D. García − *CICA − Centro Interdisciplinar de Química e Bioloxía and Departamento de Química, Facultade de Ciencias, Universidade da Coruña, A Coruña 15071, Spain;* orcid.org/0000-0002-3189-740X; Email: marcos.garcia1@udc.es

Authors

Alejandro Vila − *CICA − Centro Interdisciplinar de Química e Bioloxía and Departamento de Química, Facultade de Ciencias, Universidade da Coruña, A Coruña 15071, Spain*

Francisco G. Blandón-Cumbreras − *CIQSO − Center for Research in Sustainable Chemistry and Department of Chemistry, University of Huelva, Huelva 21071, Spain*

Mike Pauls − *Institute of Physical Chemistry, RWTH Aachen University, Aachen 52074, Germany;* orcid.org/0009-0004-3962-9639

Mauro Díaz-Abellás − *CICA − Centro Interdisciplinar de Química e Bioloxía and Departamento de Química, Facultade de Ciencias, Universidade da Coruña, A Coruña 15071, Spain;* orcid.org/0000-0003-3405-2063

Arturo Blanco-Gómez − *CICA − Centro Interdisciplinar de Química e Bioloxía and Departamento de Química, Facultade de Ciencias, Universidade da Coruña, A Coruña 15071, Spain;* orcid.org/0000-0001-7822-0423

Carlos Peinador − *CICA − Centro Interdisciplinar de Química e Bioloxía and Departamento de Química, Facultade de Ciencias, Universidade da Coruña, A Coruña 15071, Spain;* orcid.org/0000-0001-5823-6217

Patricia Remón − *CIQSO − Center for Research in Sustainable Chemistry and Department of Chemistry, University of Huelva, Huelva 21071, Spain*

Complete contact information is available at: https://pubs.acs.org/10.1021/acs.joc.5c02962

Author Contributions

The manuscript was written through contributions of all authors. All authors have given approval to the final version of the manuscript.

Notes

The authors declare no competing financial interest.

■ ACKNOWLEDGMENTS

The authors are grateful for the funding received from the MCIN/AEI/10.13039/501100011033 and ERDF *A way of making Europe* (PID2022-137361NB-I00 for C.P./M.D.G., PID2020-119992GB-I00 and PID2023-152556NB-I00 for U.P. and predoctoral contract PRE2023-001520 for F.G.B.-C.), and the Consellería de Cultura, Educación e Universidade da Xunta de Galicia (ED431C 2022/39). M.D.-A. thanks Ministerio de Universidades for his predoctoral fellowship (FPU21/06302). A.B.-G. thanks the Consellería de Cultura, Educación e Universidade da Xunta de Galicia for his postdoctoral fellowship (ED481D-2024-020). M.D.G. thanks CESGA (Xunta de Galicia) for computational time. C.B. acknowledges funding from the Federal Ministry of Education and Research (BMBF) and the Ministry of Culture and Science of the German State of North Rhine-Westphalia (MKW) under the Excellence Strategy of the Federal Government and the Länder (RWTH JPI Fellowship), as well as funding from the MKW via the NRW Rückkehrprogramm.

REFERENCES

(1) (a) Feringa, B. L.; Browne, W. R. *Molecular Switches*; John Wiley & Sons: Weinheim, 2011. (b) Dürr, H.; Bouas-Laurent, H. *Photochromism: Molecules and Systems*; Elsevier: Amsterdam, 2003. (c) Harris, J. D.; Moran, M. J.; Aprahamian, I. New Molecular Switch Architectures. *Proc. Natl. Acad. Sci. U.S.A.* **2018**, *115*, 9414−9422.

(2) For selected recent reviews, see: (a) Andreasson, J.; Pischel, U. Light-Stimulated Molecular and Supramolecular Systems for Information Processing and beyond. *Coord. Chem. Rev.* **2021**, *429*, No. 213695. (b) Wang, H.; Bisoyi, H. K.; Zhang, X.; Hassan, F.; Li, Q. Visible Light-Driven Molecular Switches and Motors: Recent Developments and Applications. *Chem.−Eur. J.* **2022**, *28*, No. e2021039061. (c) Goulet-Hanssens, A.; Eisenreich, F.; Hecht, S. Enlightening Materials with Photoswitches. *Adv. Mater.* **2020**, *32*, No. 1905966. (d) Kobauri, P.; Dekker, F. J.; Szymański, W.; Feringa, B. L. Rational Design in Photopharmacology with Molecular Photoswitches. *Angew. Chem., Int. Ed.* **2023**, *62*, No. e202300681. (e) Corra, S.; Curcio, M.; Credi, A. *Photoactivated Artificial Molecular Motors. JACS Au* **2023**, *3*, 1301−1313.

(3) For selected recent reviews, see: (a) Göstl, R.; Senf, A.; Hecht, S. Remote-Controlling Chemical Reactions by Light: Towards Chemistry with High Spatio-Temporal Resolution. *Chem. Soc. Rev.* **2014**, *43*, 1982−1996. (b) Kathan, M.; Hecht, S. Photoswitchable Molecules as Key Ingredients to Drive Systems Away from the Global Thermodynamic Minimum. *Chem. Soc. Rev.* **2017**, *46*, 5536−5550. (c) Sachini, B.; Corra, S.; Curcio, M.; Groppi, J.; Credi, A. Defying Chemical Equilibrium with Light. *Trends Chem.* **2025**, *7*, 372−383.

(4) Volaric, J.; Szymanski, W.; Simeth, N. A.; Feringa, B. L. Molecular Photoswitches in Aqueous Environments. *Chem. Soc. Rev.* **2021**, *50*, 12377−12449.

(5) (a) Liao, Y. Design and Applications of Metastable-State Photoacids. *Acc. Chem. Res.* **2017**, *50*, 1956−1964. (b) Liao, Y. Reversible Photo Control of Proton Chemistry. *Phys. Chem. Chem. Phys.* **2022**, *24*, 4116−4124.

(6) For selected reviews, see: (a) Wang, Y.; Zhang, Y.-M.; Zhang, S. X.-A. Stimuli-Induced Reversible Proton Transfer for Stimuli-Responsive Materials and Devices. *Acc. Chem. Res.* **2021**, *54*, 2216−2226. (b) Dai, X.; Gangadharappa, C.; Chen, S.; Cherif, S. E.; Gericke, C.; Yadav, B.; Pezzato, C.; Kim, D. J. Non-Equilibrium Proton Gradients for Photoenergy Conversion. *ACS Appl. Energy Mater.* **2025**, *8*, 9983−9991.

(7) For selected reviews by Aprahamian et al., see: (a) Shao, B.; Aprahamian, I. Hydrazones as New Molecular Tools. *Chem.* **2020**, *6*, 2162−2173. (b) Aprahamian, I. Hydrazone Switches and Things in Between. *Chem. Commun.* **2017**, *53*, 6674−6684. (c) Su, X.; Aprahamian, I. Hydrazone-Based Switches, Metallo-Assemblies and Sensors. *Chem. Soc. Rev.* **2014**, *43*, 1963−1981. (d) Tatum, L. A.; Su, X.; Aprahamian, I. Simple Hydrazone Building Blocks for Complicated Functional Materials. *Acc. Chem. Res.* **2014**, *47*, 2141−2149.

(8) Jan van Dijken, D.; Kovaríček, P.; Ihrig, S. P.; Hecht, S. Acylhydrazones as Widely Tunable Photoswitches. *J. Am. Chem. Soc.* **2015**, *137*, 14982−14991.

(9) Kalia, J.; Raines, R. T. Hydrolytic Stability of Hydrazones and Oximes. *Angew. Chem., Int. Ed.* **2008**, *47*, 7523−7526.

(10) See, for instance: (a) Shao, B.; Baroncini, M.; Qian, H.; Bussotti, L.; Di Donato, M.; Credi, A.; Aprahamian, I. Solution and Solid-State Emission Toggling of a Photochromic Hydrazone. *J. Am. Chem. Soc.* **2018**, *140*, 12323−12327. (b) Yang, S.; Larsen, D.; Pellegrini, M.; Meier, S.; Mierke, D. F.; Beeren, S. R.; Aprahamian, I. Dynamic Enzymatic Synthesis of γ-Cyclodextrin Using a Photoremovable Hydrazone Template. *Chem.* **2021**, *7*, 2190−2200.

(11) Barravecchia, L.; Blanco-Gómez, A.; Neira, I.; Skackauskaite, R.; Vila, A.; Rey-Rico, A.; Peinador, C.; García, M. D. "Vermellogens" and the Development of CB[8]-based Supramolecular Switches Using pH-responsive and Non-Toxic Viologen Analogues. *J. Am. Chem. Soc.* **2022**, *144*, 19127−19136.

(12) For a recent review on viologens: Striepe, L.; Baumgartner, T. Viologens and their Application as Functional Materials. *Chem.−Eur. J.* **2017**, *23*, 16924−16940.

(13) Neira, I.; Blanco-Gómez, A.; Quintela, J. M.; García, M. D.; Peinador, C. Dissecting the "Blue Box": Self-Assembly Strategies for the Construction of Multipurpose Polycationic Cyclophanes. *Acc. Chem. Res.* **2020**, *53*, 2336−2346.

(14) For recent examples on vermellogen-based (supra)molecular chemistry, see: (a) Neira, I.; Blanco-Gómez, A.; Quintela, J. M.; Peinador, C.; García, M. D. Adjusting The Dynamism Of Covalent Imine Chemistry in the Aqueous Synthesis of Cucurbit[7]uril-based [2]-Rotaxanes. *Org. Lett.* **2019**, *21*, 8976−8980. (b) Blanco-Gómez, A.; Fernández-Blanco, Á.; Blanco, V.; Rodríguez, J.; Peinador, C.; García, M. D. Thinking Outside the "Blue Box": Induced Fit within a Unique Self-Assembled Polycationic Cyclophane. *J. Am. Chem. Soc.* **2019**, *141*, 3959−3964. (c) Blanco-Gómez, A.; Neira, I.; Barriada, J. L.; Melle-Franco, M.; Peinador, C.; García, M. D. Thinking Outside the "Blue Box": from Molecular to Supramolecular pH-Responsiveness. *Chem. Sci.* **2019**, *10*, 10680−10686. (d) Cortón, P.; Wang, H.; Neira, I.; Blanco-Gómez, A.; Pazos, E.; Peinador, C.; Li, H.; García, M. D. The "Red Cage": Implementation of pH-Responsiveness within a Macrobicyclic Pyridinium-Based Molecular Host. *Org. Chem. Front.* **2021**, *9*, 81−87. (e) Cortón, P.; Fernández-Labandeira, N.; Díaz-Abellás, M.; Peinador, C.; Pazos, E.; Blanco-Gómez, A.; García, M. D. Aqueous Three-Component Self-Assembly of a Pseudo[1]rotaxane Using Hydrazone Bonds. *J. Org. Chem.* **2023**, *88*, 6784−6790. (f) Fernández-Labandeira, N.; Montes de Oca, I.; Pazos, E.; Blanco-Gómez, A.; Peinador, C.; García, M. D. Modulating The Dimensions Of Rectangular Hydrazone-Based Bispyridinium Macrocyclic Receptors. *J. Org. Chem.* **2025**, *90*, 8621−8627.

(15) An initial version of this work was deposited at ChemRxiv: Vila, A.; Blandón-Cumbreras, F. G.; Pauls, M.; Díaz-Abellás, M.; Blanco-Gómez, A.; Peinador, C.; Remón, P.; Bannwarth, C.; Pischel, U.; García, M. D. Photovermellogens: Minimalistic Pyridinium-Based Metastable Acylhydrazone Photobases for Operation in Aqueous Media. *ChemRxiv*, **2025**. (submission date: 22−11−2025) .

(16) See supplementary information for further information.

(17) It should be noted that, due to the fast exchange on the NMR timescale for the species involved in the acid−base processes (e.g. *E*-$\mathbf{P}_a\mathrm{H}^+ + \mathrm{H_2O} \rightleftharpoons$ *E*-$\mathbf{P}_a + \mathrm{H_3O}^+$), the spectra reflects pH-dependent averaged resonances.

(18) Grimme, S.; Brandenburg, J. G.; Bannwarth, C.; Hansen, A. Consistent structures and interactions by density functional theory with small atomic orbital basis sets. *J. Chem. Phys.* **2015**, *143*, No. 054107.

(19) Barone, V.; Cossi, M. Quantum Calculation of Molecular Energies and Energy Gradients in Solution by a Conductor Solvent Model. *J. Phys. Chem. A* **1998**, *102*, 1995−2001.

(20) The lack of observed isomerization of the conjugate bases *E*-$\mathbf{P}_{a-c}$ can be rationalized by the destruction of the HB motif upon deprotonation, and the consequent destabilization of the conjugate bases *Z*-$\mathbf{P}_{a-c}$. Nevertheless, the overlapping of spectroscopic absorption features for *E*/*Z*-$\mathbf{P}_{a-c}$ (see main text), further hampers the potential *E*→*Z* photoisomerization in basic media.

(21) Bannwarth, C.; Yu, J. K.; Hohenstein, E. G.; Martínez, T. J. Hole−Hole Tamm−Dancoff-Approximated Density Functional Theory: a Highly Efficient Electronic Structure Method Incorporating Dynamic and Static Correlation. *J. Chem. Phys.* **2020**, *153*, No. 024110.

(22) Yu, J. K.; Bannwarth, C.; Hohenstein, E. G.; Martínez, T. J. *Ab Initio* Nonadiabatic Molecular Dynamics with Hole−Hole Tamm−Dancoff Approximated Density Functional Theory. *J. Chem. Theory Comput.* **2020**, *16*, 5499−5511.

(23) Steinbach, P.; Bannwarth, C. Combining Low-Cost Electronic Structure Theory and Low-Cost Parallel Computing Architecture. *Phys. Chem. Chem. Phys.* **2024**, *26*, 16567−16578.

(24) Bannwarth, C.; Ehlert, S.; Grimme, S. GFN2-xTB—An Accurate and Broadly Parametrized Self-Consistent Tight-Binding Quantum Chemical Method with Multipole Electrostatics and Density-Dependent Dispersion Contributions. *J. Chem. Theory Comput.* **2019**, *15*, 1652−1671.

(25) Ehlert, S.; Stahn, M.; Spicher, S.; Grimme, S. Robust and Efficient Implicit Solvation Model for Fast Semiempirical Methods. *J. Chem. Theory Comput.* **2021**, *17*, 4250−4261.

https://doi.org/10.1021/acs.joc.5c02962
J. Org. Chem. 2026, 91, 6559−6565

(26) Martin, R. L. Natural transition orbitals. *J. Chem. Phys.* **2003**, *118*, 4775−4777.
(27) Yin, T.-T.; Zhao, Z.-X.; Yu, L.-Y.; Zhang, H.-X. Theoretical study on the thermal *cis-Trans* isomerization of novel acylhydrazone photoswitches. *Org. Electron.* **2017**, *48*, 154−164.
(28) Reimann, M.; Teichmann, E.; Hecht, S.; Kaupp, M. Solving the Azobenzene Entropy Puzzle: Direct Evidence for Multi-State Reactivity. *J. Phys. Chem. Lett.* **2022**, *13*, 10882−10888.
(29) Kortekaas, L.; Browne, W. R. The Evolution of Spiropyran: Fundamentals and Progress of an Extraordinarily Versatile Photochrome. *Chem. Soc. Rev.* **2019**, *48*, 3406−3424.

https://doi.org/10.1021/acs.joc.5c02962
J. Org. Chem. 2026, 91, 6559−6565